THE JOURNAL OF PHYSICAL CHEMISTRY B LETTERS

2006, *110,* 22968−22970
Published on Web 11/02/2006

Small Molecule Directed Aggregation of a Heme Peptide on Gold: An STM Study

James D. Satterlee and Ursula Mazur*

Department of Chemistry and Materials Science Program, Washington State University, Pullman, Washington 99164-4630

Received: August 16, 2006; In Final Form: October 11, 2006

Microperoxidase 11 was adsorbed on Au(111) from basic aqueous solutions containing pure heme peptide and co-added stoichiometric amounts of exogenous neutral and ionic ligands. The addition of small molecules to MP11 produced different aggregate structures that were easily differentiated by STM. In the absence of a complexing agent, the MP-11 formed large clusters of metallopeptide molecules on the gold surface. With neutral imidazole in solution the MP11 aggregated into regular elongated structures (nano-épis) on the substrate. When S^{2-} is used as coupling agent, single heme peptide molecules are isolated with identifiable porphyrin ring and substructure in the peptide chain.

Introduction

Protein aggregation is frequently associated with undesirable properties, such as expression of insoluble recombinant proteins or neurodegenerative diseases including Alzheimer's, Parkinson's, and the prion diseases.[1,2] However, another aspect of protein chemistry involves functional aggregation, in which aggregation is required for proper protein function. Specifically, understanding how aggregation of heme-based oxygen sensing and signaling proteins regulates their normal function is important for understanding cellular processes in organisms as diverse as humans and bacteria.[3] At present neither of these processes is understood, yet doing so could facilitate their control.

We have begun studying the functional aggregation of heme oxygen-sensing/signaling proteins in solution and adsorbed on surfaces using scanning tunneling microscopy (STM). Here we report initial studies using microperoxidase-11 (MP11), a truncated version of equine cytochrome *c* consisting of an undecapeptide ($Val_{11}-Gln_{12}-Lys_{13}-Cys_{14}-Ala_{15}-Gln_{16}-Cys_{17}-His_{18}-Thr_{19}-Val_{20}-Glu_{21}$) covalently bound to heme-c (Figure 1).[4] MP11 is well known for its use as a model for heme proteins, as well as in biosensors, biofuel cells, and as a biophotodiode, and demonstrates nonspecific aggregation on surfaces that reduces device efficiency.[6,7]

The results presented here reveal that it is possible to systematically control MP11 aggregation on Au(111), and more significantly, we observe in the STM images, *for the first time*, structural details of both the heme ring and the polypeptide substructure in individual MP11 molecules. The different aggregation structures are readily differentiated by STM and are controlled by selection of exogenous ligand for MP11. This ligand-mediated aggregation is the first systematic control of surface aggregation that has been identified for any metallomolecule.

* Corresponding author. E-mail: umazur@wsu.edu

Experimental Section

MP11 was purchased from Sigma-Aldrich and used as received. Reagent grade imidazole and sodium sulfide nonahydrate were acquired from Sigma-Aldrich and Fisher Chemicals, respectively. The heme peptide solutions in different ligand environments were adsorbed on Au(111) by exposing freshly annealed gold substrates to a few drops of the desired aqueous (MilliPore Milli Q-purified water, 18 MΩ) mixture for 15−30 s and wicking off the excess liquid with an edge of a Kimwipe tissue. Samples were then dried under a gentle flow of an inert gas for 15 min and subsequently imaged. Ligand-free MP11 solution was 1.0×10^{-6} M. A few pure MP11 STM samples were prepared with small (<10%) coadded volumes of ethanol or methanol. The resultant images were not significantly different from those obtained from MP11 in pure water. Reference imidazole and imidazole plus MP11 solutions that were employed were stoichiometric, 5.0×10^{-6} M at pH = 9.51. Pure NaS_2 and approximately equal amounts of sodium sulfide and MP11 formed 1.2×10^{-6} M solutions with pH equal to 11.2. The formation of monomeric imidazole and sulfide-ligated MP11 species in solutions used for STM imaging was verified by UV−visible spectroscopy using a Cintra (GBC Scientific) dual beam spectrometer interfaced to a Gateway desktop computer running GBC Spectral software.[8]

STM imaging was performed in air and in argon atmosphere at 21 °C using a Molecular Imaging Picoscan outfitted with a 1-micron scanner. Constant current images are reported after a flattening procedure. STM tips were prepared from 0.25-mm $Pt_{0.8}Ir_{0.2}$ wire by electrochemical etching. Models of MP11 were generated from the X-ray crystal coordinates (PDB ID: 1HRC) of equine cytochrome *c*[4], manipulated and displayed in DS Viewer Pro (Accelrys). The model shown in Figure 1 was created be deleting all entries in the 1HRC.pdb file except for the coordinates of amino acids 11−21 and heme. The only other modification from the crystal coordinates was rotation of the Val11 side chain by 130° around the Cα−Cβ bond, reflecting

10.1021/jp065312o CCC: $33.50

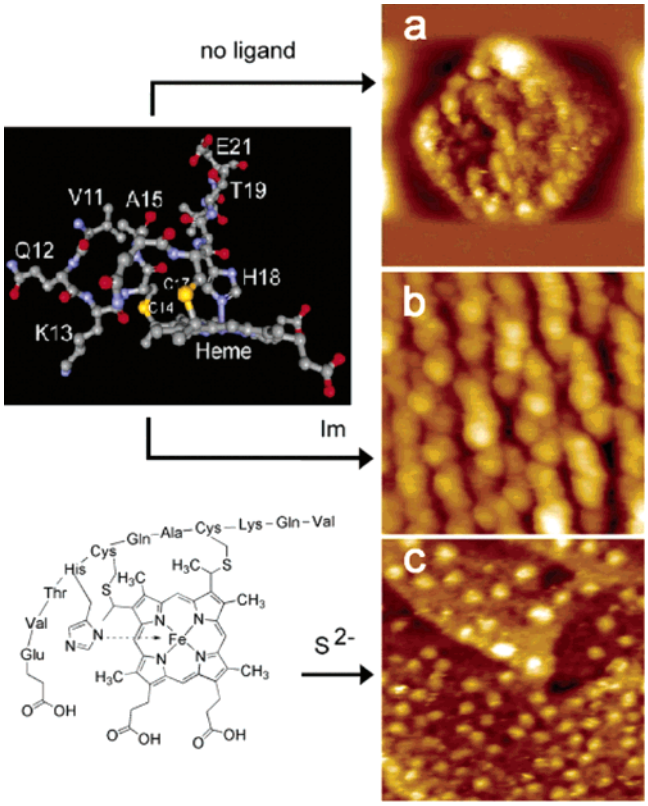

Figure 1. Medium resolution 50 × 50 nm^2 STM images of MP11 adsorbed onto Au(111) from different fluid solutions. All images were obtained under ambient conditions. MP-11 without complexing ligands forms round clusters about 40−50 nm in diameter and 12 nm high (a). Image was obtained at a bias voltage of +900 mV and a tunneling current of 40 pA. In the presence of imidazole the MP-11 adsorbs as elongated aggregate structures 6 nm wide ∼15 nm long and 2.2 nm in height (b). Scan parameters were +800 mV bias and tunneling current of 120 pA. In the presence of an ionic ligand, S^{2-}, MP11 adsorbs as isolated single molecules 2.4 nm × 1.5 and 0.85 nm high (c). Image was obtained at a bias voltage of −800 mV and a tunneling current of 100 pA. MP11 space-filled model was constructed from the crystal structure (PDB ID:1HRC[4]) guided by the MP-11 solution structure.[9]

the extent of conformational flexibility found in the solution NMR structure of MP11.[9]

Results and Discussion

Figure 1 displays STM images obtained from MP11 adsorbed on Au(111) from different solutions. In the absence of added ligands MP11 forms mostly large regular clusters of individual molecules on the metal surface, Figure 1a. These clusters averaged ∼30−50 nm in diameter and were ∼12 nm high. This type of peptide aggregation is not unexpected since, in general, when proteins are brought into contact with a surface they tend to assemble into disorganized aggregates that may contain hundreds of molecules.

When the Au substrate is exposed to a solution containing stoichiometric amounts of MP11 and imidazole, regular elongated molecular stacks or chains were observed. These "nano-épis[9]" (∼6 nm wide, ∼15 nm long, ∼2.2 nm high) were uniformly distributed over the entire substrate surface, Figure 1b. This result is reproducible and contrasts with the solution behavior of MP11 with exogenous ligands, such as CN^-, imidazole, and ammonia where the heme peptide is predominantly monomeric.[10,11] Based upon the apparent dimensions (∼6 nm width, ∼15 nm length, ∼ 2.2 nm height) of the nano-épis (Figure 1b), it is likely that their discernible subunits are either

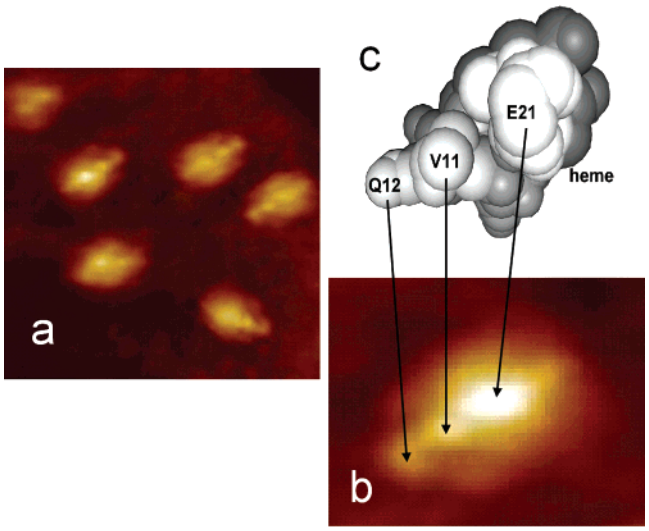

Figure 2. High-resolution 10 × 10 nm image of MP-11 adsorbed on Au(111) from aqueous solution containing a stoichiometric amount of Na_2S (a). The image was obtained at 21 °C under argon atmosphere with −600 mV bias and 100 pA tunneling current. An enlarged single MP11-S molecule from image (a) is depicted in (b). Space-filling model of MP11-S oriented similarly as the molecules in the lower image (b) is depicted in (c). Arrows indicate the topographical features of the model that correlate to the submolecular features in the MP11-S image.

dimers or trimers, although at this time the mode of aggregation is unclear.

Figure 1c shows that images of the size of individual isolated MP11 molecules are obtained when S^{2-} is used as a heme ligand in the precursor solution. Optical spectra document this ligation and concomitant conversion to a 6-coordinate low-spin MP11-S complex.[8] It is well-known that MP11 ligation to form 6-coordinate complexes eliminates self-aggregation in solution (see refs 10, 11, and references therein).

The possibility that these structures are Au−S_x clusters was discounted because, when freshly annealed gold substrate was exposed to a NaS_2 solution, under similar experimental conditions as the MP11-S system, no discernible topographical features were seen. Stable adlayers of sulfur can be formed on Au(111) under potential control[12,13] − an experimental condition not employed in our work. S^{2-} ligation of MP11 thus insures complete disaggregation of MP11-S in the precursor solution, which is clearly transferred to the Au surface. As a bridge between heme and Au(111) it also creates an efficient conduction pathway, thereby enhancing STM imaging. The MP11 orientation detected in the images can be deduced by knowing that thiols and disulfides are regularly employed to facilitate molecular adsorption onto metal surfaces.[14] Our hypothesis is that a sulfide ligand binding to heme-iron acts as a bridge between heme and the Au surface, stereospecifically orienting MP11 on the surface in an orientation in which the heme is approximately parallel to the Au surface: peptide−heme−Fe−S−Au. Additional stabilization between MP11-S and the gold surface may come from the heme carboxylates, since COO^- is known to adsorb to gold in a horizontal (flat) orientation or pendant to the surface, as would be the case for our model.[15,16]

Details of the internal structure and orientation of individual MP11-S molecules are seen in the high-resolution images in Figures 2 and 3. In acquiring and interpreting this data, we have considered possible tip-effects which are known to induce reorientation and distortions such as enhanced corrugations of

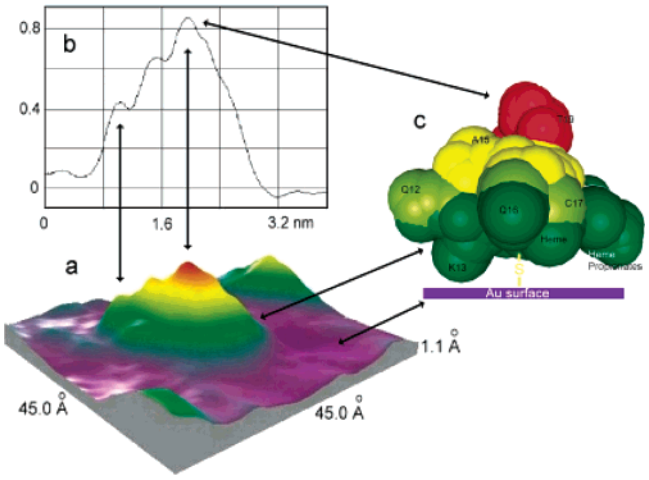

Figure 3. STM image of a single MP11-S molecule on Au (111) is portrayed in (a). The height profile of an MP11 molecule (taken from STM data) crossing its long axis at maximum intensity is depicted in (b). The space-filled model silhouette of MP11 in (c) presents height variations within MP11-S. Correlations are indicated by arrows.

the adsorbed species.[17,18] We observed no significant changes in image resolution in the many STM data that we have collected. Submolecular structural details of adsorbed MP11 are clearly recognized in Figure 2a. These features include the elongated orientation of the polypeptide chain above the heme ring.

By comparing an enlarged view of an MP11 molecule, Figure 2b, with the corresponding orientation of a space-filling MP11 model, Figure 2c, correlations become apparent that reveal strong correspondence not only in structural details but also in dimensions. Both the image and the model have strikingly similar features corresponding to submolecular topography details of the MP11 model (vide infra). These are indicated by labels and arrows between parallel features in the model and the image. The length and width dimensions of the adsorbed MP11 monomers are 2.4 nm × 1.5 nm and are identical to the MP11 model structure measuring ∼2.5 nm × ∼1.3 nm.[4] These lateral dimensions agree well with the NMR structure[10] and the crystal structure of equine cyt.[4]

While very high-resolution STM images of simple porphyrins are well known,[19] this quality of resolution has not been previously reported for any biomolecule, including those metalloproteins previously examined.[20,21]

The cross-section profile of the image replicates structural variations in the model MP11-S structure remarkably well. This is clearly demonstrated by comparing Figures 3a−c. The apparent height of individual molecules, 0.85 nm (Figure 3b), however, does not correlate well with the model's actual vertical (height) measurements of 1.5 nm. Disagreement between molecular heights measured in STM and those based on crystallography constitute a general phenomenon in STM, especially for imaging biological molecules.[22]

The "highest (brightest) spot" in the molecular images in Figures 2 and 3a indicate tunneling enhancement in the region of the axial heme ligand (His18), reflecting the well-known propensity (from solution NMR studies) for electron density delocalization from the paramagnetic low spin iron into the proximal histidine orbitals in heme proteins.[23] The two additional bright features diagonally in line with "highest spot" can be attributed to Val11/Ala15 and Gln12 residues, respectively (Figure 2a and 2b). In solution, the N-terminal sequence, Val11-Gln12-Lys13, is very flexible, but on the surface one would expect that physisorption of Lys13 restricts motion of the N-terminus. Amino acids are known to physisorb in the zwitterionic form on gold.[24] The image in Figure 2a shows that the highest areas (brightest spots) of the MP11 polypeptide are linear, whereas the model suggests that the Gln12 white spot is off the diagonal of the topological high spots. The STM images indicate that Lys13 may have reoriented for physisorption to the surface, thereby altering the orientation of Gln12 compared to the model. This is consistent with the dynamical behavior of the MP11 N-terminus found in the solution structure.

Further work, currently in progress, is devoted to improving resolution of MP11-S monomers. We are studying the temporal formation of the MP11−imidazole nano-épis and exploring application of electrochemical STM. We are also expanding these types of experiments to other heme peptides.

Acknowledgment. We thank the National Institutes of Health GM47645 and the National Science Foundation CHE 0234726 and CHE 0555696 for supporting this work. We also thank Marian Marston and Lesley Crawford for their assistance with some of the STM measurements.

Supporting Information Available: Epitaxial Au(111) substrate preparation and corresponding STM images. This material is available free of charge via the Internet at http://pubs.acs.org.

References and Notes

(1) Glatzel, M.; Giger, O.; Braun, N.; Aguzzi, A. *Cur. Mol. Med.* **2004**, *4*, 355−359.
(2) Kokalj, S.; Stoka, V.; Kenig, M.; Gunear, G.; Turk, D.; Zerovnik, E. *Acta Chim. Slov.* **2005**, *52*, 27−33.
(3) Reedy, C. J.; Gibney, B. *Chem. Rev.* **2004**, *104*, 617−649.
(4) Luo, Y.; Brayer, G. V. *J. Mol. Biol.* **1990**, *214*, 585−595. The Research Collabotatory for Structural Bioinformatics PDB: Berman, H. M.; Westbrook, J.; Feng, Z.; Gilliland, G.; Bhat, T. N.; Weissig, H.; Shindyalov, I. N.; Bourne, P. E. *Nucleic Acids Res.* **2000** *28*, 236−242; www.pdb.org.
(5) Castner, D. G.; Ratner, B. D. *Surf. Sci.* **2002**, *500*, 28−60.
(6) Lee, J. B.; Kim, D. J.; Choi, J. W.; Koo, K. K. *Mater. Sci. Eng.* **2004**, *C24*, 79−81.
(7) Norde, W. In *Physical Chemistry of Biological Interfaces*; Baszkin, A., Norde, W., Eds.; Marcel Dekker: New York, 2000; pp 115−137.
(8) Satterlee, J.D.; Mazur U., to be published.
(9) épis (French) for "ear of wheat"; wordreference.com/fren/epis
(10) Mondelli, R.; Scaglioni, L.; Mazzini, S.; Bolis, G.; Ranghino, G. *Magn. Reson. Chem.* **2000**, *38*, 229−240.
(11) Satterlee, J. D. *Inorg. Chim. Acta* **1983**, *79*, 195−197.
(12) Vericat, C.; Vela, M. E.; Andreasen, G.; Salvarezza, R. C.; Vazquez, L.; Martin-Gago, J. A. *Langmuir* **2001**, *17*, 4919−4924.
(13) Gao, X.; Zhang, Y.; Weaver, M. J. *J. Phys. Chem.* **1992**, *96*, 4156−4159.
(14) Bonanni, D.; Alliata, D.; Andolfi, L; Bizzarri, A. R.; Cannistraro, S. In *Surface Science Research Developments*; Norris, C. P.; Ed.; Nova Science Pub.: Hauppauge, NY, 2005; pp 1−73.
(15) Yu, K. H.; Rhee, J. M, Lee, Y.; Lee, K.; Yu, S. C. *Langmuir* **2001**, *17*, 52−55.
(16) Gyarfas, B.; Wiggins, B.; Zosel, M.; Hipps, K. W. *Langmuir* **2005**, 21, 919−923.
(17) Sasaki, N.; Tsukada, M. *Adv. Mater. Res.* **2000**, *2*, 1−41.
(18) Taylor, M. E.; Golen, B.; McKinnon, A. W.; Rosolen, G. C.; Gray, S. M.; Welland, M. E. *Appl. Surf. Sci.* **1993**, *67*, 228−34.
(19) Hipps, K. W.; Scudiero, L. *J. Chem. Ed.* **2005**, *82*, 704−711.
(20) Chi, Q.; Zhang, J.; Jensen, P. S.; Christensen, H. E. M.; Ulstrup, J. *Faraday Discuss.* **2006**, *131*, 181−195.
(21) Bizzarri, A. R.; Andolfi, L.; Stchakovsky, M.; Cannistraro, S. *J. Nanotechnol. Online (AZojono)* **2005**, *1*, 1−12; www.azonano.com.
(22) Scudiero, L.; Barlow, D. E.; Mazur, U.; Hipps, K. W. *J. Am. Chem. Soc.* **2001**, *123*, 4073−4080.
(23) La Mar, G. N.; Satterlee, J. D.; de Ropp, J. S. In *The Porphyrin Handbook*; Kadish, K. M., Smith, R. G., Eds; Academic Press: San Diego, 2000; Vol 5, pp 185.
(24) Lieberg, B.; Lundstrom, I.; Wu, C. R.; Salaneck, W. R. *J. Colloid Interface Sci.* **1985**, *108*, 123−132.